UNILAG Journal of Medicine, Science and Technology

MODELLING AND ANALYSIS OF THREE PHASE CONTROLLED RECTIFIERS USING PIVOTAL FUNCTION TECHNIQUE

Kalunta[1], F. O., Akinbulire[2], T. O. and Okafor[3], F. N.
Electrical/Electronics Engineering Department, University of Lagos, Nigeria
[1]felka3@yahoo.co.uk, [3]cfrankok@yahoo.com

Abstract
This paper describes the extension of pivotal function approach to deriving the mathematical representation of the input current of a controlled three phase bridge rectifier circuit. The basis is that a single thyristor and its associated rectifier circuits could be modelled as a pivotal function which relates the input voltage and current with load resistance. In the conduction region the thyristor behaves as a double P-N junction diode, which implies that it could be modelled as a pivotal function with the conduction interval controlled by a gate firing pulse. On this projection is based the development of a thyristor controlled rectifier model in this paper beginning with the mathematical expression of a thyristor current. The model equation was derived in a manner as to include or exclude the effect of source inductance for flexible applications. Considering the effect of source inductance resulted in a non-linear second order ordinary differential equation with the inverse pivotal function as the second coefficient. The model was also modified to cater for cases involving unbalanced three phase supply voltages. Simulation result on the studied circuit based on the derived model expression compared with its counterpart from Simpower simulation has established that the pivotal function technique reflects properly the regulating behavior of a thyristor. The derived model was deployed in analyzing the waveforms and harmonic profile of the distorted input current of the studied circuit at different firing angles. The result has established that the derived model will further enhance the analysis of controlled rectifiers in resonance studies.

Keywords: Controlled Rectifiers; Harmonic Distortion; Pivotal Function; Resonance; Thyristors.

1. INTRODUCTION
Semiconductor rectifiers abound in the power industry; they constitute the power stage of most non-linear power equipment and therefore require appropriate model expressions in power system analysis and design. The major obstacle is the time varying nature of most power converters arising from their switching characteristics. Several attempts were made by many researchers including Udomsuk *et al*. (2011) and Md Hasan *et al.* (2012) to eliminate the switching action and achieve a time invariant model where classical control theory can easily be applied. The first is the generalized state space averaging (SSA) employed by Emadi (2004a) in the analyses of power converters involved in DC distribution systems and Emadi (2004b) in the analysis of rectifiers in single phase AC

distribution systems. Another method widely used for AC system analysis is the Direct – Quadrature axes (DQ) Transformation theory whereby the rectifier is modelled as a transformer on d – and q – axes, and other network elements expressed as rotating frames. The DQ method has been employed by Areerak *et al.* (2008) in stability analysis, and in the modelling of three-phase controlled and uncontrolled rectifiers by Chaijaroenudomrung *et al*. (2010). Ruttanee *et al.* (2011) on the other hand reported a combination of SSA and DQ transformation methods (DQ + SSA) in deriving a dynamic model of controlled three phase rectifier feeding an uncontrolled buck converter in a DC distribution system.

In all these techniques, the focus is on the modelling of the entire power network to determine its low frequency behaviour while neglecting the harmonic frequencies injected into the network as a result of the non-linear characteristics of these rectifiers. It makes the assessment of harmonic distortion and its associated resonance phenomenon impossible. It is more important to derive an isolated model for the rectifier if this can be achieved. In that regard, an attempt was made by Kazeem *et al.* (2005) to model the converters as non-linear loads by application of Fourier theory on the switching function of a single-phase ideal diode bridge rectifier to generate a frequency spectrum of sine waves. However this model was limited to single-phase rectifier and does not portray the exponential characteristics of a practical diode. Pejovic and Kolar (2008) also derived an analytical expression for rectifier input current, but on the basis of the piecewise linear model of the diode and specific power schematics. These modelling techniques are therefore not suitable for resonance studies, where knowledge of the actual injected harmonic spectrum is necessary.

A recent research effort by Kalunta and Okafor (2015) effectively modelled the input current of three phase uncontrolled rectifier circuits based on the use of a pivotal function. In this model, the exponential characteristics of a practical diode are retained and the rectifier topological variations are reflected in a Table of rectifier parameters. High frequencies injected into the system by the rectifier which contribute significantly to system resonance were adequately captured in simulations based on this modeling approach. However, scope of the study was limited to uncontrolled rectifiers assembled from semiconductor diodes. The emergence of thyristor-controlled devices like static var compensators (SVC) and controlled rectifiers has underscored the need to adapt the pivotal function approach to their power quality assessment. Some industrial applications of three-phase controlled rectifiers are induction furnaces, DC arc furnaces and speed control of DC motors. The concept of induction heating employed in the industrial furnaces as demonstrated by Ahmed *et al*. (2009) involves conversion of the AC current from the power source to DC using a controlled rectifier. Controlled rectifiers are composed of thyristors with their gates fired at specified angles for the purpose of regulating the output. The mathematical model of controlled rectifiers is significant in system design and analysis especially in electrical networks prone to resonance hazards.

In the conduction region the thyristor behaves as a double P-N junction diode, with the conduction interval controlled by a gate firing pulse. By extension, a double P – N junction semiconductor thyristor could likewise be modelled as a pivotal function except that the conduction interval is modified in accordance with the firing angle. On this projection is based the development of a thyristor controlled rectifier model described in this paper. It begins with the mathematical expression of a thyristor current and further extension to the input current of three-phase controlled rectifiers using Fig. 2 as reference circuit. The results of this analysis are compared with its counterpart from Simpower simulation. The adaptation of pivotal function approach to modelling controlled rectifiers will further enhance their analysis during resonance studies.

2. REVIEW OF PIVOTAL FUNCTION TECHNIQUE

The basis of the pivotal function approach is that a practical diode, a P – N junction semiconductor could be modelled as a pivotal function in order to retain its exponential characteristics which is lacking in the piecewise linear model. According to Kalunta and Okafor (2015), a practical diode comprising an ideal diode in series with a finite forward resistance R_f and voltage drop as depicted in Fig. 1 could be modelled as a closed loop gain having R_f in the feedback loop. This model also represents its incremental conductance.

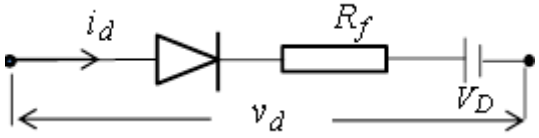

Fig. 1: Schematic representation of a practical semiconductor diode

The non-linear characteristics of an ideal semiconductor diode is represented by its exponential equation (1), (Acha and Madrigal, 2001)

Diode current $$i_d = I_s \exp\left(\frac{ev_d}{bT} - 1\right) \quad (1)$$

Supposing we define an exponential coefficient, $\beta = \frac{e}{bT}$

The diode voltage is then expressed as,

$$v_d = \frac{1}{\beta}\left[1 + \ln\left(i_d / I_s\right)\right] \quad (2)$$

where: I_s - reverse saturation current, i_d – diode current, e = 1.602 x 10-19 (electronic charge),

b = 1.38 x 10^{-23} (Boltzmann constant), v_d – applied voltage, T – Ambient Temperature (Kelvin)

Differentiating both sides of (2) with respect to i_d gives,

$$\frac{dv_d}{di_d} = \frac{1}{\beta i_d} \tag{3}$$

Hence for an ideal diode,

$$\frac{di_d}{dv_d} = \beta i_d \quad [\Omega^{-1}] \tag{4}$$

A practical diode comprises an ideal diode in series with a finite forward resistance R_f and voltage drop, V_D as indicated in Fig. 1. Supposing a sinusoidal supply voltage, v_s, is connected to the diode terminals, and Kirchhoff's Voltage Law applied,

$$v_s = V_D + i_d R_f + v_d$$

$$v_s = V_D + i_d R_f + \frac{1}{\beta}\left[1 + \ln\left(i_d / I_s\right)\right] \tag{5}$$

Differentiating both sides of (5) with respect to i_d gives,

$$\frac{dv_s}{di_d} = R_f + \frac{1}{\beta i_d}$$

$$\frac{di_d}{dv_s} = \frac{\beta i_d}{1 + \beta i_d R_f} \tag{6}$$

where: source voltage $v_s = \sqrt{2} V_{ph} \sin(\omega t)$

The input current of a diode over the conduction interval is therefore,

$$i_d = \int \frac{\beta i_d}{1 + \beta i_d R_f} \omega \sqrt{2} V_{ph} \cos(\omega t) dt \quad \forall \qquad 0 \le \omega t < \pi \tag{7}$$

ω – power frequency (radians/seconds),

V_{ph} – magnitude of supply voltage,

t – time (seconds)

Introducing a new variable *P* to represent the incremental conductance of a rectifier, different rectifier topologies could be represented by the following unified model expression,

$$P = \frac{di_{in}}{dv_{in}} = \frac{\beta i'_{in}}{A + \beta i'_{in} R'_L} \tag{8}$$

P is tagged as the *pivotal function* model of the rectifier,

A is a constant while i'_{in} and R'_L are the characteristic parameters described in a Table arising from the application of specific modelling procedure on different rectifier configurations (Kalunta and Okafor, 2015). The initial values of the current are obtained from the instantaneous values of applied voltage at points of commutation.

3. A TYPICAL THREE PHASE CONTROLLED RECTIFIER CIRCUIT

This section describes the actual topology of the studied circuit as applied in the design of the power stage of induction furnace and DC arc furnace. A typical three-phase controlled rectifier is a three-phase, 2-Way, 6-Pole (3ph2W6P) rectifier composed of thyristors as the switching device with their gates fired at specified angles as shown in Fig. 2. The two pulses in each current cycle are fired simultaneously at angles α_1 and α_2. The firing order corresponds with the numbering of thyristors in each phase (α_1 - firing angle for T_1 and T_2, α_2 - firing angle for T_4).

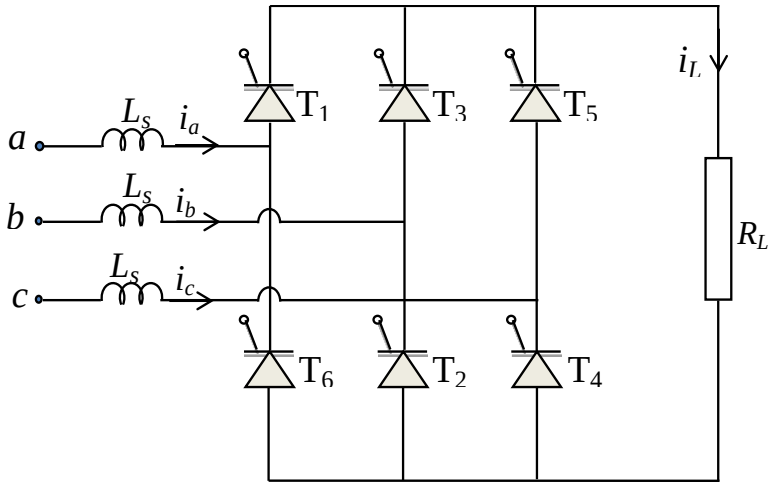

Fig. 2: The schematic design of fully controlled three phase full wave bridge rectifier showing the source inductance and resistive dc load, R_L.

Its power quality assessment could be conducted using the pivotal function technique described in the previous section.

4. METHODOLOGY

4.1 Adaptation of Pivotal Function Model to Thyristors

A practical thyristor could then be considered as a double P – N junction semiconductor in series with a finite forward resistance R_f and voltage drop, V_D. Application of (1) in a simple thyristor circuit supplying a resistive load, R_L, produces the required model expression.

$$v_s = \frac{2}{\beta}\ln\left[\frac{i_{th}}{I_s}\right] + i_{th}R_f + i_{th}R_L + V_D \tag{9}$$

$$P = \frac{di_{th}}{dv_s} = \frac{\beta i_{th}}{2 + \beta i_{th}R_L'} \tag{10}$$

$R_L' = R_f + R_L$, and source voltage $v_s = \sqrt{2}V_{ph}\sin(\omega t)$.

P is the pivotal function for modelling of thyristor,

R_L - Load Resistance

i_{th} - thyristor current

The thyristor current based on (10) and defined over the conduction intervals is,

$$i_{th}(t) = \begin{cases} \int \frac{\beta i_{th}}{2 + \beta i_{th}R_L'}\omega\sqrt{2}V_{ph}\cos(\omega t)dt & \forall \quad \alpha \le \omega t < \alpha + \lambda \\ 0 & \forall \quad \alpha + \lambda \le \omega t \le 2\pi \\ i_{th}(\omega t - 2\pi) & \forall \quad \omega t > 2\pi \end{cases} \tag{11}$$

Note: $i_{th} > 0 \;\forall\; \omega t \le \pi$, $\lambda = \pi - 2\alpha$, $\alpha_{\max} = \pi/2$, V_{ph} - phase voltage and α - thyristor firing angle, ω - power frequency (radians/seconds)

4.2 Procedure for the Modelling of Three-phase Controlled Rectifier

In this section, the pivotal model of a single thyristor is applied to the fully controlled three-phase bridge rectifier shown in Fig 2. This was achieved by means of the following algorithm

i. A schematic diagram of the actual rectifier circuit design is required showing the connection of the thyristors and the load.
ii. The output voltage waveform is examined to determine the conduction interval of the thyristors during the first cycle. The conduction interval for each input cycle is defined by the no load output voltage.
iii. For flexible applications, an equivalent circuit of the thyristor bridge circuit is drawn first from the given schematic diagram. The purpose is to derive a model

which excludes the source inductance. For three phase circuits, the equivalent circuit is drawn for each phase showing the phase voltage and flow path of input currents for each conduction interval phase.

iv. By the application of Kirchhoff's voltage and current laws, an expression for the input voltage v_{in} in terms of the input current i_{in} is derived.

v. Differentiation with respect to the input current is carried out to obtain the expression similar to the pivotal function, and the characteristic parameters are therefore extracted from this expression.

vi. The supply circuit comprising the source voltage and inductance is later connected to the rectifier module while circuit laws and pivotal function derived in (v) are applied to obtain the dynamic model of rectifier input current.

vii. For the purpose of analyzing the waveform and distortion profile of the rectifier input current, numerical solution of the derived model expression coded in a Matlab programming tool is obtained using a step size of $0.1ms$, phase voltage of $V_{ph} = 415V$ and load resistance of $R_L = 100\Omega$. Other parameters, $\beta = 38.7 Coulombs/Kelvin$, $\omega = 315 rad/s$, $I_s = 10^{-3} A$, $R_f = 10\Omega$, $L_s = 30mH$ and initial values of input current, $i_{in}(0) = -1.0$ for half wave, $i_{in}(0) = 1.0$ for full wave.

In this study, an undistorted sinusoidal input is assumed in the simulation with fixed input voltage and fixed source inductance.

4.3 Derived Model Expressions

The procedure outlined in the previous section were applied to Fig. 2 to obtain the model expression of phase 'a' current of the controlled rectifier bridge, which represents a balanced three-phase condition resulting from a system of balanced and undistorted three phase supply voltage V_{ph} applied to the rectifier. By application of (9), which represents the voltage across a single thyristor, as well as Kirchhoff's Voltage Law on Fig. 2, the model equation of phase 'a' current of the controlled rectifier bridge based on pivotal function technique while neglecting the source inductance was derived as follows,

$$v_{ab} = 2V_D + \frac{4}{\beta}\ln\left[\frac{i_a - I_s}{I_s}\right] + \frac{3}{2}R_f(i_a - I_s) + R_L(i_a - 3I_s) \qquad (12)$$

and upon differentiation,

$$\frac{dv_{ab}}{di_a} = \frac{4}{\beta(i_a - I_s)} + (\frac{3}{2}R_f + R_L)$$

$$\frac{di_a}{dv_{ab}} = \frac{\beta i'_a}{4 + \beta i'_a R'_L} \tag{13}$$

$A = 4$, $i'_a = (i_a - I_s)$, and $R'_L = \frac{3}{2} R_f + R_L$, $v_{ab} = \sqrt{2} V_{ph} \sin(\omega t)$

$$i_a = \begin{cases} 0 & \forall \quad 0 < \omega t \le \alpha_1 \\ \int P \omega \sqrt{2} V_{ph} \cos(\omega t) dt & \forall \quad \alpha_1 < \omega t \le \alpha_2 \\ -\int P \omega \sqrt{2} V_{ph} \cos(\omega t + \frac{2\pi}{3}) dt & \forall \quad \alpha_2 < \omega t \le \pi \\ -i_a(\omega t - 2\pi) & \forall \quad \omega t > \pi \end{cases} \tag{14}$$

Note: $i_a > 0 \ \forall \ \omega t \le \pi$, $\alpha_2 = \alpha_1 + \pi/3$.

where the pivotal function, $P = \frac{\beta i'_a}{4 + \beta i'_a R'_L}$ (15)

The two pulses in each cycle of the input current were fired simultaneously at angles α_1 and α_2.

The inclusion of leakage inductance L_s of the supply transformer into the circuit results in a non-linear second order ordinary differential equation for the rectifier input current with the inverse pivotal function as its second coefficient as stated in (16).

$$\frac{d^2 i_a}{dt^2} = \begin{cases} \frac{\omega}{L_s} \sqrt{2} V_{ph} \cos(\omega t) - \frac{1}{L_s P} \frac{di_a}{dt} & \forall \quad \alpha_1 + \varphi \le \omega t < \alpha_2 \\ -\frac{\omega}{L_s} \sqrt{2} V_{ph} \cos(\omega t + \frac{2\pi}{3}) - \frac{1}{L_s P(t)} \frac{di_a}{dt} & \forall \quad \alpha_2 \le \omega t < \alpha_1 + 2\pi \end{cases} \tag{16}$$

$i_a > 0 \ \forall \ \omega t \le \pi$, $i_a = -i_a(\omega t - \pi) \ \forall \quad \omega t > \pi$

The unbalanced three phase equivalent of (16) was also derived and represented by the current at *k*-th phase,

$$\frac{d^2 i_k}{dt^2} = \begin{cases} \frac{\omega}{L_{sk}} \sqrt{2} V_k \cos[\omega t + 2\pi(1-k)/3] - \frac{1}{L_{sk} P} \frac{di_k}{dt} & \forall \quad \alpha_1 + \varphi + 2\pi(k-1)/3 \le \omega t < \alpha_2 + 2\pi(k-1)/3 \\ -\frac{\omega}{L_{sk}} \sqrt{2} V_k \cos[\omega t + 2\pi(2-k)/3] - \frac{1}{L_{sk} P} \frac{di_k}{dt} & \forall \quad \alpha_2 + 2\pi(k-1)/3 \le \omega t \le \alpha_1 + 2\pi + 2\pi(k-1)/3 \end{cases} \tag{17}$$

$i_k > 0 \ \forall \ \omega t \le \pi$, $i_k = -i_k(\omega t - \pi) \ \forall \quad \omega t > \pi$

where: the phase $k \in \{1,2,3\}$, V_k – k-th phase voltage and L_{sk} – transformer leakage inductance for phase k.

The three-phase model expression is applicable to circumstances involving unbalanced three phase supply voltages. These second order non-linear equation do not possess any closed form solution but numerical methods could be applied to generate the data which represents the instantaneous currents. These data could be plotted to obtain the current waveform, and also subjected to Fourier analysis to obtain the harmonic currents.

4.4 Model Verification

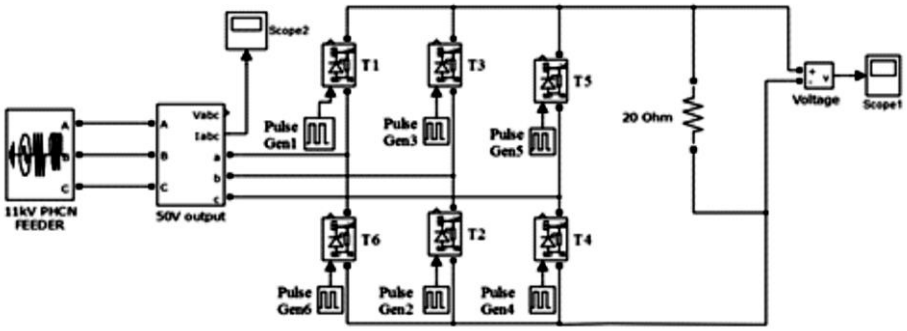

Fig. 3: Simpower model schematic diagram of fully controlled three-phase full wave bridge rectifier showing the source inductance and resistive load

Simpower simulation of the studied circuit was conducted under the same conditions as stipulated using the schematic diagram of the rectifier as shown in Fig. 3. The purpose is to determine the current waveform, total harmonic distortion (THD) and current magnitudes at different thyristor firing angles.

The data generated by this simulation were analyzed to produce the distorted input current waveform at the phase 'a' and the frequency spectrum. The waveforms are so timed in a manner as to avoid the transient response and select only steady state values. The steady state is attained when a cycle of the waveform is within the period of 0.02s interval. The graphical results of both simulations based on the proposed model and Simpower model are displayed for further comparison.

5. RESULTS AND DISCUSSIONS

This section presents the result of the theoretical analyses on the controlled rectifier under study in terms of waveforms and harmonic tables. The results from simulations based on the proposed pivotal function approach and Simpower are also compared. The plotted values are obtained from the instantaneous data representing the distorted input current. Fig. 4 indicates a disparity between the pivotal technique and simpower simulation model

in terms of shape of current waveform at a firing angle $\alpha_1/5$. The pivotal current is symmetrical about its central axis coinciding with that of the applied voltage while the Simpower current is skewed to the right of this axis because the Simpower simulation is based on the piecewise linear model of the semiconductor device. The minimum and maximum limits of firing angle are shown in Fig. 5.

Current waveforms for different thyristor firing angles illustrating the regulating action of the thyristor are displayed in Fig. 6 for a single thyristor circuit and Fig. 7 for the rectifier circuit under study. The current decomposition begins with the second pulse down to the first pulse and the point at which the second pulse disappears seem to coincide with B ($\alpha_1 = \pi/2$). The thyristor current decreases towards zero from its maximum value as the firing angle is increased from zero to the maximum value $\alpha_1 = \pi/2$ (see Fig. 5).

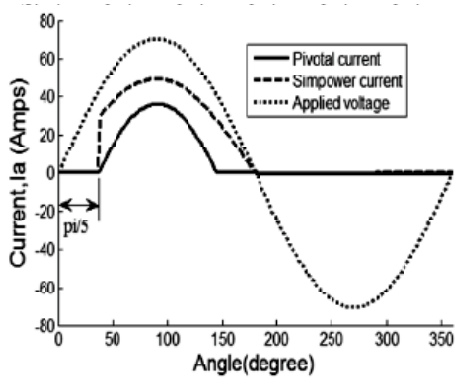

Fig. 4: Thyristor current waveform from simulations using Simpower and pivotal Technique respectively

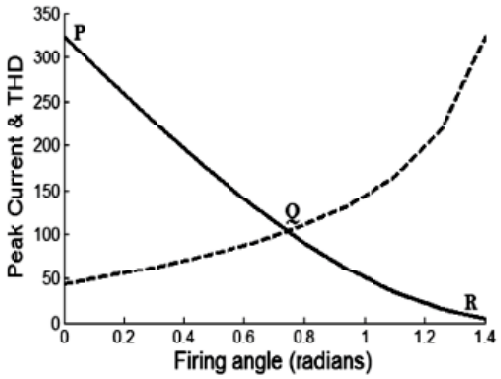

Fig. 5: Variation of Peak Current & THD with firing angle in a single thyristor circuit

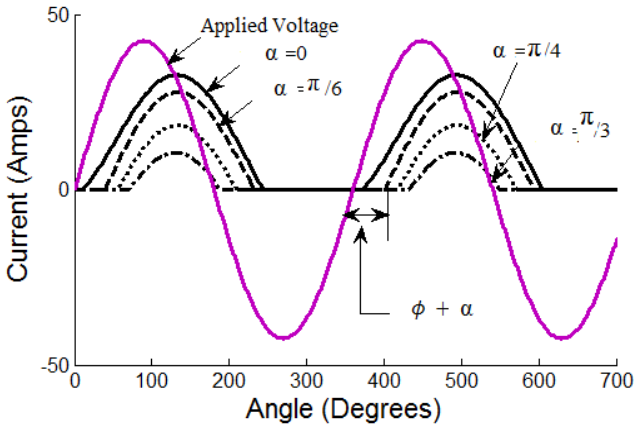

Fig. 6: Current waveforms for different firing angles in a single thyristor circuit with series reactance

The Total Harmonic Distortions (THD) computed at different firing angles starting from $\pi/3$ shows that there is relative stability before B and rapid increase in THD after B where the second pulse has varnished. The region A – B gives an optimum operating range of the device because it maintains a stable distortion profile of THD = 30%. This implies that the optimum range of angles to be adopted for effective firing of the thyristor is $\pi/3 \leq \alpha_1 < 2\pi/5$. Thus the current distortion at any point in the region could be uniformly represented with a harmonic table (Table 1) computed by Fast Fourier Transform of discrete instantaneous currents. The figures in this table indicate the frequencies injected into the system by this rectifier which also need to be mitigated with a filter.

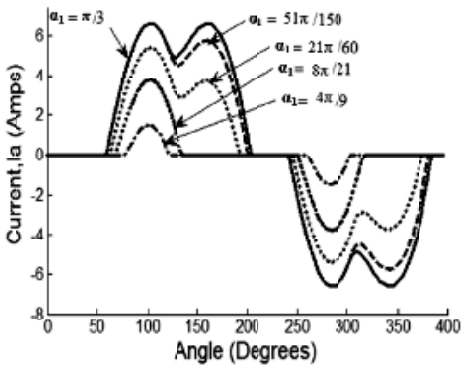

Fig. 7: Current waveforms for different firing angles in a 3ph2W6P controlled rectifier

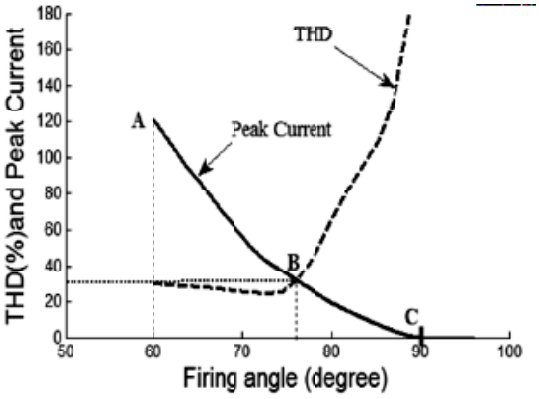

Fig. 8: Variation of Peak Current & THD with firing angle in a 3ph2W6P controlled rectifier

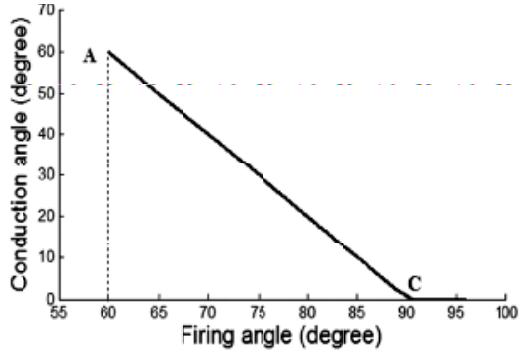

Fig. 9: Variation of conduction angle with firing angle in a 3ph2W6P controlled rectifier

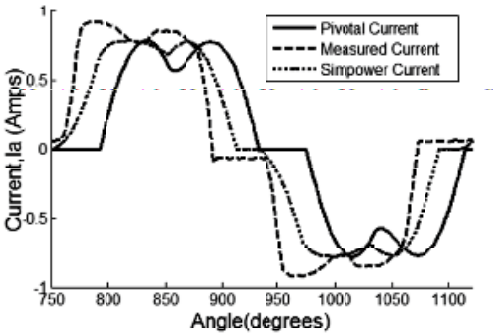

Fig. 10: Distorted input current waveform of 3ph2 W6P controlled rectifier at zero firing angle

Information displayed in Figure 8 is that C, representing $\alpha_1 = \pi/2$, is the maximum limit for the firing angle of the first pulse since the current magnitude decreases to zero at C. This is also confirmed in Fig. 9 where the conduction angle is observed to decrease linearly from its maximum value at A ($\alpha_1 = \pi/3$) to zero at C. Extrapolating the line to vertical axis reveals the linear relationship between the conduction angle and firing angle as $\lambda = \pi - 2\alpha_1$. The results of simulation at zero firing angle are comparable to that of a diode bridge circuit as shown in Fig. 10.

Table 1: Harmonic table for the pivotal current of 3Ph2W6P controlled rectifier

Harmonic Order (*h*)	**Harmonic magnitude, A_n (%)**			
	$\alpha_1 = 60^o$	$\alpha_1 = 65^o$	$\alpha_1 = 70^o$	$\alpha_1 = 75^o$
1	100	100	100	100
2	0.27	0.24	0.33	1.03
3	15.83	13.76	12.77	28.64
4	0.38	0.38	0.36	0.24
5	15.26	16.42	16.62	12.91
6	0.58	0.57	0.48	0.43
7	10.70	9.73	7.07	1.50
8	0.55	0.49	0.34	0.23
9	7.73	6.40	4.10	3.04
10	0.49	0.39	0.28	0.04
11	5.42	5.00	4.67	2.47
12	0.47	0.46	0.41	0.18
13	4.87	4.91	4.11	0.23
14	0.51	0.50	0.40	0.15
15	4.57	4.36	3.04	0.90
THD (%)	29.4	**28.0**	25.0	31.8

A closer look at Table 1 reveals that the distortion profile changes with the firing angle as well as the magnitude of each harmonic component. The strength of higher order harmonics decreases at a faster rate at higher values of firing angle (also represented by the A – B section of THD curve in Fig. 8). This may appear as elimination process for high order harmonics, but ironically the waveform is almost lost at high values of firing

angle. In order to strike a balance, an optimum operational firing angle which can reduce the harmonic content as well as retain the waveform is desired (preferably $\alpha_1 = 65^o$).

6. CONCLUSION

This paper describes an attempt to develop a pivotal function approach to the modelling of different controlled rectifier configurations while using a three-phase fully controlled bridge rectifier as reference circuit. Simulation of rectifier configurations based on this approach has clearly captured all the significant harmonic frequencies contained in the rectifier input current. It has also established that the level of harmonic content differs for various firing angles. The uniqueness in this model is the effectiveness in the evaluation of distortion profile of induction furnace and DC arc furnaces in three-phase power distribution systems better than in modern power system simulation softwares like SimPower and ETAP. The derived model expression retains the exponential characteristics of the P – N junction semiconductor device. Simpower software employs the piecewise linear model and does not permit the kind of flexibility in the rectifier supply voltage as applied in the pivotal function model. The impact on distortion level created by the ohmic heating of diode bridge, leakage current, load resistance, distorted supply voltage, phase shift can easily be examined using this approach.

REFERENCES

Acha, E. and Madrigal, M. (2001). Power systems harmonics: Computer modelling and analysis. John Wiley and Sons Ltd., Chichester England, pp. 52 – 53.

Ahmed M., Masoud M. and El-Sharkawy A. (2009), "Design of a Coreless Induction Furnace for Melting Iron", *International Conference on Communication, Computer and Power, Muscat*, 15th – 18th February 2009, pp. 102 – 106.

Areerak K-N., Bozhko S., Asher G.M. and Thomas D.W. (2008), "Stability Analysis and Modelling of AC-DC System with Mixed Load Using DQ-Transformation Method", *IEEE International Symposium on Industrial Electronics*, Cambridge UK, 29 June-2 July 2008, pp. 19 – 24swx.

Carpinelli G., Iacovone F., Varilone P. and Verde P. (2003). "Single Phase Voltage Source converters: Analytical Modeling for Harmonic Analysis in Continuous and Discontinuous Current Conditions", *International Journal* of Power and Energy Systems, 23 (1): 37 – 48.

Chaijaroenudomrung K., Areerak K-N and Areerak K-L (2010); Modeling of Three Phase Controlled Rectifier using a DQ Method, *International conference on Advances in Energy Engineering (ICAEE 2010), Beijing, China*, 19th – 20th June 2010, pp. 56 – 59.

Emadi, A. (2004). "Modeling and Analysis of Multi-converter DC Power Electronic Systems

using the Generalized State-Space Averaging Method," *IEEE Trans. on Indus. Elect.*, 51 (3): 661 – 668.

Emadi, A. (2004). "Modeling of Power Electronic Loads in AC Distribution Systems using the Genearlized State-Space Averaging Method", *IEEE Trans. on Indus. Elect.*, 51 (5): 992-1000.

Kalunta F. O. and Okafor F. N., "Modeling of Rectifiers for Resonance Studies: A Pivotal Approach", *Proceedings of the Joint IEEE International Symposium on Electromagnetic Compatibility and EMC Europe*, Dresden Germany, 16th – 22nd August, 2015, pp 1380 – 1387.

Kazeem, H. A., Albaloshi A. A., Al-Jabri A. S., and Al-Saidi K. H. (2005) "Simple and advanced models for calculating single phase diode rectifier Line-side harmonics", World Academy of Science, Engineering and Technology journal, 9: 179 – 183.

Md Hasan K., Rauma K., Luna A., Candela J., and Rodriguez P., "Harmonic Resonance Study for Wind Power Plant**",** *International Conference on Renewable Energies and Power Quality*, Santiago de Compostela, Spain, 8th to 30th March 2012.

Pejovic P. and Kolar J. W. (2008), "Exact Analysis of Three Phase Rectifiers with constant Voltage Loads", *IEEE Transaction on circuits and on circuits and systems II*: Express Briefs, 55 (8): 743 – 747.

Ruttanee P., Areerak, K-N. and Areerak K-L. (2011), Averaging Model of a Three-Phase Controlled Rectifier Feeding an Uncontrolled Buck Converter, *World Academy of Science, Engineering and Technology Journal*, 60: 345 – 352.

Udomsuk S., Areerak K-N. and Areerak K-L., "Mathematical Model of a Single-Phase Uncontrolled Rectifier Feeding a Buck Converter", *European Journal of Scientific Research*, 50 (1): 89 – 98.